

# $\kappa$ -Carrageenan Associated with Fructose/Glycerol/Water LTTM: Toward Natural Thermosensitive Physical Gels

Benoit Caprin, Guadalupe Viñado-Buil, Guillaume Sudre, Xavier P. Morelle, Fernande Da Cruz-Boisson, Aurélie Charlot,\* and Etienne Fleury



Cite This: <https://doi.org/10.1021/acssuschemeng.2c04437>



Read Online

ACCESS |

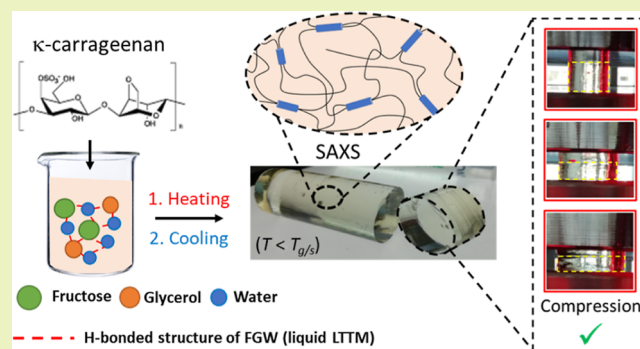
Metrics & More

Article Recommendations

Supporting Information

**ABSTRACT:**  $\kappa$ -Carrageenan was combined to a natural low-transition temperature mixture composed of fructose, glycerol, and water in a 1:1:5 molar ratio (FGW) to generate fully biobased physical gels through a simple method. The resulting gels can be easily prepared in various shapes. As for their hydrogel analogues, the rheological characterization of FGW-based samples evidenced thermosensitive gelation, attributed to the formation of aggregated H-bonded helices composed of  $\kappa$ -carrageenan chains. FGW-based gels exhibit a gel–sol transition temperature ( $T_{g/s}$ ) higher than the one of hydrogels with recoverable and reversible viscoelastic properties upon successive heating/cooling cycles. SAXS analysis revealed a more extended conformation of chains in FGW that leads to more physical cross-linking junction zones within the materials. Such peculiar spatial internal organization provides a mechanical reinforcement demonstrated by compression tests. In conclusion, the use of the FGW solvent allows for designing  $\kappa$ -carrageenan physical gels with enhanced thermal and mechanical properties.

**KEYWORDS:**  $\kappa$ -carrageenan, low-transition temperature mixture, organogels, thermo-sensitivity



## 1. INTRODUCTION

In the context of sustainable development, polysaccharides remain a powerful and tantalizing resource for biomass valorization since they can be used to generate eco-friendly materials. In this context, such natural polymers have been combined with deep eutectic solvents (DESs), just through a simple mixture, usefully exploited to obtain fully biobased and biosafe materials with relevant and tunable properties.<sup>1</sup> The interest is to benefit from the unique attributes synergistically provided by the combination of natural polymers (reduced environmental impact, renewable origin, non-toxicity, and so forth) with DES solvents, more specifically their biosafe properties, their organized character, and the large versatility they provide in terms of the final macromolecular structure. The preparation of these novel solvents is simple since DESs come from the mixture of two (or more) H-bonded low-cost molecules. When no eutectic point can be clearly identified, such mixtures are classified as low-transition temperature mixtures (LTTMs). In particular, natural DES (NaDESs) can be conceived from biobased and biosafe precursors. For instance, guar gum, a vegetal galactomannan, was combined to various choline chloride (ChCl)-based DESs and physical gels with elastic behavior and relevant ionic transport properties were formed from ChCl–urea/guar mixtures.<sup>2</sup> Xanthan gum was also described as a potential gelator of ChCl-based DESs.<sup>3</sup>

The authors proved that the addition of water was required to obtain physical gels. It is also reported that xanthan gum NaDES-based gels exhibit a larger thermal operating window compared to hydrogels due to the involvement of water in the supramolecular structure of the NaDES.<sup>4</sup> Despite the prominent interest to explore LTTMs in the polysaccharide field, the design of materials including carrageenans has not been reported yet. Carrageenans, linear sulfated polysaccharides, are mainly extracted from red algae (Rhodophyceae). Carrageenan chains consist of D-galactopyranose units alternately linked by  $\alpha$ -1,3 and  $\beta$ -1,4 glycosidic bonds. The repeating units are most often disaccharides and are generally distinguished by their degree of sulfation and by the presence or absence of a 3,6-anhydro bridge on the  $\beta$ -1,4-linked galactose unit. The three mostly studied carrageenans are  $\kappa$ ,  $\iota$ , and  $\lambda$ -carrageenan.  $\kappa$ -Carrageenan is particularly interesting since it not only finds applications in food, cosmetic, and pharmaceutical industries but it forms hard gels in aqueous

Received: July 26, 2022

Revised: October 20, 2022

## 1. Polysaccharide dispersion ➔ 2. Thermal gelation ➔ 3. Physico-chemical characterization\*

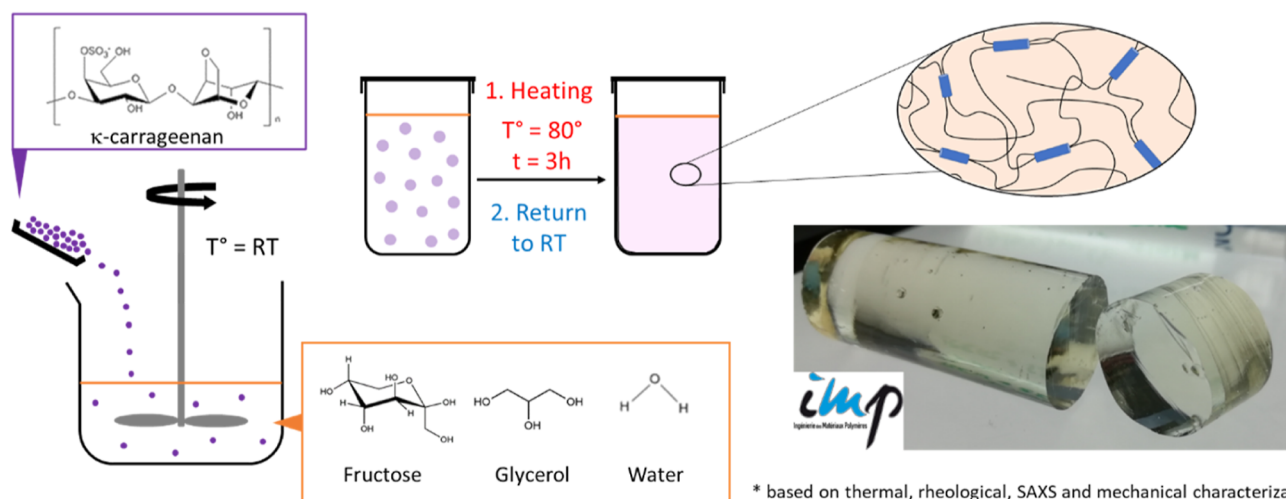


**Figure 1.** Illustration of the two-step procedure of  $\kappa$ -carrageenan/FGW gels: (1) dispersion of  $\kappa$ -carrageenan at RT, (2) heating at 80 °C for 3 h and gelation by cooling down to RT. The same procedure was applied to obtain hydrogels. (3) Picture of the  $\kappa$ -carrageenan/FGW gel.

medium.<sup>5</sup> It is accepted that the gelation of  $\kappa$ -carrageenan in water is achieved by a two-step thermo-dependent mechanism. Upon cooling, a coil-to-helix transition occurs, followed by the aggregation of helices, resulting in gelation.<sup>6</sup> This gelation has been investigated by rheological and micro differential scanning calorimetry (DSC), which allowed to determine thermal transitions: from solution to gel ( $T_{s/g}$ ) and from gel to solution ( $T_{g/s}$ ).<sup>7</sup> The influence of the nature of the solvent on the thermal transitions was also examined by Yang *et al.* by additions of sucrose or ethanol in water solutions.<sup>8,9</sup> Their investigation emphasized that the nanostructure of the gel was affected by the solvent.

In this context, we propose herein a new study dealing with the association of  $\kappa$ -carrageenan and a novel green solvent, namely, a neutral low LTTM, composed of bio-sourced and non-toxic molecules: fructose (F), glycerol (G), and water (W). Indeed, we recently reported by means of DSC, rheology, and NMR spectroscopy that FGW in 1:1:5 molar ratio (subsequently named FGW) behaves as a cooperatively H-bonded supramolecular structure leading to a stable solvent identified as LTTM exhibiting a unique and low  $T_g$  and an outstanding microbiological stability.<sup>10</sup> Moreover, this composition was industrially implemented to efficiently extract bioactive substances from plants for cosmetic applications.<sup>11</sup> Due to its appealing advantages in terms of structuration, polarity, and ability to develop synergetic interactions between its compounds, we pursue as a statement of hypothesis that FGW constitutes a well-suited solvent to generate, when mixed with  $\kappa$ -carrageenan, soft materials with improved thermo-reversible properties and reinforced mechanical behavior, compared to water-based systems.

In this work, we evidence for the first time the straightforward formation of physical gels based on the incorporation of  $\kappa$ -carrageenan in FGW. In particular, we successively (i) investigate their physico-chemical properties through thermal analysis, (ii) use rheological measurements to characterize the formation of gels and to underpin the thermal dependence of the gelation mechanism, (iii) use small angle X-ray scattering (SAXS) experiments to elucidate their internal structure, and (iv) perform compression tests in order to validate their mechanical response. The properties of

analogous  $\kappa$ -carrageenan hydrogels were systematically analyzed and compared with our novel system, in order to gain insights into the role of the FGW solvent in the structuration of the gels, which is shown to dictate the final properties. To the best of our knowledge, this is the first study dealing with soft materials resulting from  $\kappa$ -carrageenan and a fully biobased LTTM.

## 2. EXPERIMENTAL SECTION

**2.1. Materials.** Fructose (powder,  $M = 180.16$  g/mol, purity > 99%) provided by Danisco and glycerol (liquid at 25 °C,  $M = 92.09$  g/mol, purity > 99.5%) acquired from Oleon were used without any further purification. Deionized water (18 M $\Omega$ -cm) obtained from a Veolia Aquadem system was used as the third component to obtain the FGW LTTM according to the recently described method.<sup>10</sup>  $\kappa$ -Carrageenan was provided by Roth and was used without any further purification. Its water uptake ( $\approx 7$  wt %) and thermal decomposition temperature ( $\approx 250$  °C) were measured by thermogravimetric analysis (Figure S1). Its molar mass determined by size exclusion chromatography is  $M_w \approx 6.0 \times 10^5$  g/mol with a dispersity of 1.3 (Figure S2). Elementary analysis conducted by inductively coupled plasma-atomic emission spectrometry confirms that the counter ion of the  $\kappa$ -carrageenan used is potassium since equivalent molar quantities of sulfur and potassium were obtained (data not shown). The structure of  $\kappa$ -carrageenan was confirmed by <sup>1</sup>H NMR analysis (Figure S3).

**2.2. Preparation of the Samples.** The preparation is based on two main steps. The first step corresponds to the dispersion of  $\kappa$ -carrageenan into FGW at room temperature (RT), under slow mechanical stirring. RT allows to limit water evaporation that can disturb the H-bonds of FGW. For concentration of polysaccharide higher than 15 g/L, the volume of liquid and the height of the rotor were adjusted to ensure an efficient stirring, while preventing the formation of bubbles in these highly viscous solutions. The water content of  $\kappa$ -carrageenan was considered for the calculation of the total amount of polysaccharide. The resulting turbid  $\kappa$ -carrageenan/FGW mixture was stirred for 30 min. The second step consists of thermal-induced gelation. The mixture was gently poured into a cylindrical recipient to prevent the formation of bubbles. The recipient was then capped and put in a temperature-controlled oven at 80 °C for 3 h, in which the sample progressively became transparent. The thermal-induced gelation process of  $\kappa$ -carrageenan occurred during the cooling phase down to RT. The as-formed FGW-gels were pushed out of the recipient and transparent cylindrical

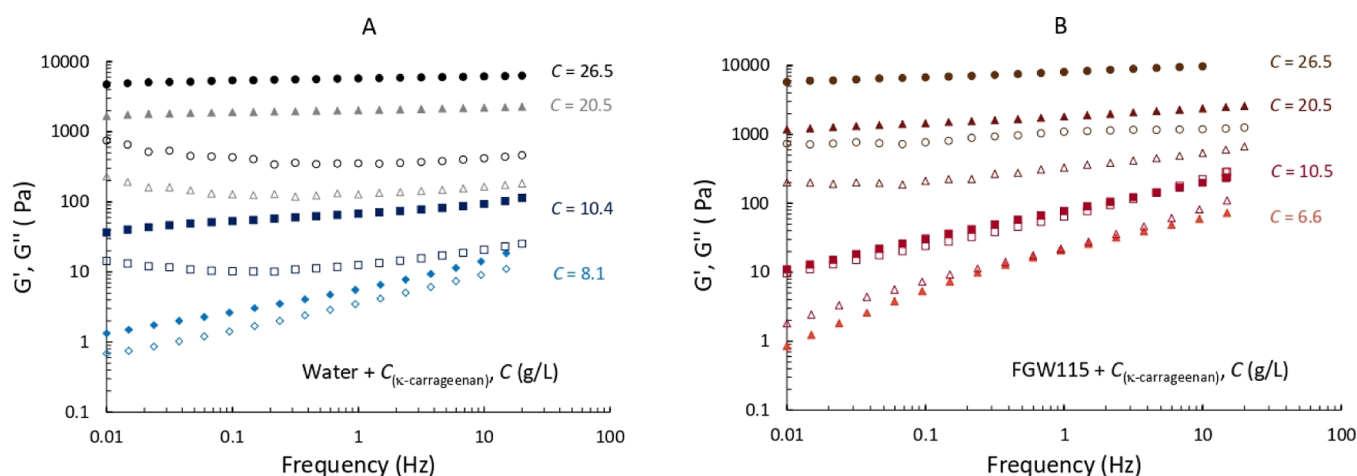


**Figure 2.** Frequency dependence of  $G'$  (filled symbols) and  $G''$  (open symbols) at different concentrations ( $C$  in g/L) of  $\kappa$ -carrageenan in water in blue (A) and in FGW in red (B) at 20 °C.

samples were finally obtained as illustrated in Figure 1. The same procedure was applied to generate hydrogels by replacing the FGW solvent with deionized water. By convenience, the carrageenan concentration is usually discussed in mass fractions (wt %) in the literature. However, in this study, the concentration is expressed in g/L as FGW is denser than water ( $d = 1.3$ ).

**2.3. Characterizations.** **2.3.1. Differential Scanning Calorimetry.** DSC analyses were carried out on a DSC-Q22 device (TA Instruments). Samples were placed in aluminum hermetic pans at RT. Thermal analyses were performed under nitrogen flow (50 mL/min), and samples were submitted to 4 temperature cycles with a ramp rate of 10 °C/min: (1) from 25 °C down to −140 °C; (2) from −140 °C up to 100 °C; (3) from 100 °C down to −140 °C; and (4) from −140 °C up to 25 °C. The glass transition temperature ( $T_g$ ) was determined from the second heating ramp, and the midpoint of the thermal transition was considered. The melting temperature ( $T_m$ ) value of hydrogels was collected from the first heating run, and the maximum of the thermal transition was considered.

**2.3.2. Rheology.** Shear viscosity ( $\eta$ ) measurements were carried out on a DHR2 controlled stress rheometer (TA Instruments) operating in flow mode and using two different geometries according to the viscosity of the mixtures: (i) an aluminum cone/plate geometry (diameter 40 mm, angle 2°, gap 52  $\mu$ m) for viscosities higher than 2 Pa·s and (ii) an aluminum concentric cylinder geometry (bob diameter  $\times$  length: 28.03  $\times$  42.11 mm, cup diameter 30.36 mm) for viscosities lower than 2 Pa·s. The temperature was precisely controlled using a high-power Peltier system. Dynamic viscoelastic properties were determined with the same rheometer using a plate/plate geometry (diameter 40 mm, gap 460  $\mu$ m). All dynamic rheological data were checked as a function of strain amplitude to ensure that the measurements were performed in the linear domain. Typically, the applied strain during the dynamical measurements was settled at 1%. Temperature sweep on gels was realized in the same conditions ( $F = 1$  Hz, strain = 1%). The samples were carefully loaded on the Peltier plate regulated at 20 °C and covered with a home-made cover to prevent evaporation. The temperature was then increased using a controlled temperature ramp to a maximum temperature depending on the analyzed sample (see Results and Discussion part). Then, the temperature was decreased using the same ramp to examine the reversibility with temperature. For the highest concentrations of  $\kappa$ -carrageenan in FGW, multiple thermal cycles (heating and cooling) were performed. All rheological data were processed with Trios, TA Instruments software.

**2.3.3. SAXS Analysis.** SAXS measurements were performed at the European Synchrotron Radiation Facility (ESRF, Grenoble, France) on the D2AM beamline. Samples were placed between 250  $\mu$ m Kapton foils stuck on 1.6 mm-thick washers. Measurements were performed on samples equilibrated at either 20 or 80 °C. The incident

photon energy  $E$  was set to 17.000 keV ( $\Delta E/E = 10^{-4}$ ). The SAXS intensity was collected using a 2D D5 detector, which was placed at a sample-to-detector distance of  $D = 1.57$  m, leading to a  $q$ -range from 0.01 to 0.2  $\text{\AA}^{-1}$ . The two-dimensional data were obtained by considering the detector geometry and its flat field response. The position of the direct beam was determined with attenuators. The  $q$ -calibration was performed, thanks to a silver behenate standard. The corrected two-dimensional data were averaged azimuthally to obtain intensity versus scattering vector  $q$  [ $q = (4\pi/\lambda) \cdot \sin(\theta)$ , where  $2\theta$  is the scattering angle and  $\lambda$  is the incident wavelength]. Finally, the scattering data were corrected for the scattering from the empty cell (Kapton windows) and normalized by the thickness and attenuation of the samples. The contribution from the solvent (FGW or water) was subtracted.

**2.3.4. Compression Tests.** Compression measurements were performed on a double-column Instron universal testing machine at RT with a 500 N load cell. The cylindrical gel samples (12 mm height, 20 mm diameter) were set on the lower plate and compressed using the upper plate. The compression was conducted at a constant rate of 1 mm/min to obtain engineering stress–engineering strain curves. The compression experiments were conducted in three replicates for each gel system.

## 3. RESULTS AND DISCUSSION

**3.1. Preparation of the Samples.** Based on the literature dealing with  $\kappa$ -carrageenan hydrogels,<sup>12</sup> the gels formed with the ternary biobased FGW mixture or deionized water as the solvent were prepared according to a straightforward method described in the Experimental Section (Section 2.2). At high  $\kappa$ -carrageenan concentration ( $C = 26.5$  g/L = 2 wt % in FGW and 2.65 wt % in water), transparent soft materials with a macroscopically gel-like behavior were obtained without further processing (see picture in Figure 1). The resulting FGW-gels can be easily prepared under various shapes. Compared to the hydrogels, FGW-gels appear less slippery and less prone to syneresis and exhibit a better long-lasting physical stability without FGW exudation with time. This good dimensional stability can be ascribed to favorable and strong enough interactions (mainly H-bonds) between polysaccharide chains and the FGW solvent (see *vide infra*). Another crucial point is that FGW-based gels display an excellent microbiological stability compared to their hydrogel analogues. To conclude, an easy-to-implement and robust preparation protocol was used to obtain fully biobased gels based on polysaccharide and this natural LTTM mixture.

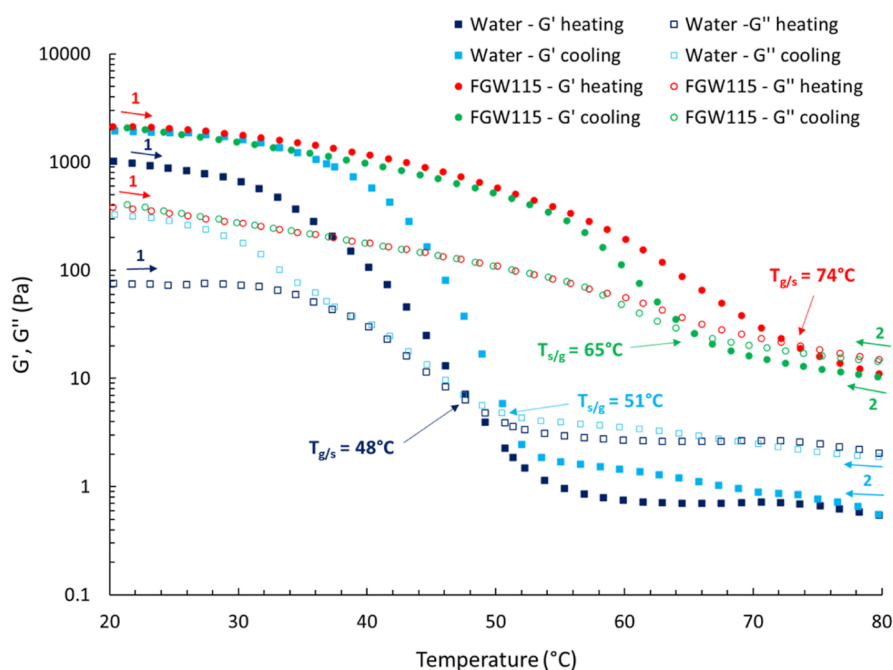


**Figure 3.** Evolution of the storage  $G'$  (filled symbols) and loss  $G''$  (open symbols) moduli as a function of temperature during a heating (1) and cooling (2) rate ( $2\text{ }^{\circ}\text{C}/\text{min}$ ),  $C = 20.5\text{ g/L}$  of  $\kappa$ -carrageenan in FGW (red and green symbols) and in water (blue and light blue symbols). The thermal transitions directly indicated in the figure correspond to the crossover point of  $G'$  and  $G''$ .

As recently described, the solvent FGW, classified as a natural LTTM, is characterized by a single and low glass transition temperature ( $T_g$ ) at  $-80\text{ }^{\circ}\text{C}$ .<sup>10</sup> DSC analyses were then applied to evaluate the impact of  $\kappa$ -carrageenan addition on FGW thermal properties. Examples of the thermogram are given in Figure S4, for a gel prepared in FGW, in comparison with the corresponding hydrogel. It appears that during the heating cycles, the hydrogel presents at  $7\text{ }^{\circ}\text{C}$  a thermal event attributed to the melting of iced water when temperature varies from  $-140\text{ }^{\circ}\text{C}$  to  $100\text{ }^{\circ}\text{C}$ , whereas the FGW-gel only exhibits a  $T_g$  at  $-79\text{ }^{\circ}\text{C}$ , related to the  $T_g$  of FGW. The presence of such a unique  $T_g$  value reflects the monophasic character of the mixture and shows that polysaccharide chains do not deeply disturb the intrinsic organization of the FGW solvent. We can note that no other thermal transition can be clearly identified in these DSC thermograms. Interestingly, the DSC analysis shows that the FGW-based samples are not subjected to any phase transition related to water, which extends their operating temperature range.

**3.2. Rheological Characterization.** Rheological properties of  $\kappa$ -carrageenan-based systems were investigated. First, the evolution of viscosity with shear rate, in water and in FGW, was examined at low concentrations ( $C < 12\text{ g/L}$ ) (Figure S5). No macroscopical gel-behavior is observed either in water or in FGW. For  $C < 5\text{ g/L}$ , the aqueous solutions exhibit a Newtonian plateau. A shear-thinning behavior is observed for larger concentrations. Conversely, FGW-based mixtures display a shear-thinning behavior even at low concentrations ( $0.6\text{ g/L}$ ). At this concentration, the viscosity of the FGW sample is 2 decades higher than the water-based one. This can be attributed first to the intrinsically higher viscosity of FGW but also to the formation of peculiar interactions between the  $\kappa$ -carrageenan chains and/or a different chain conformation in FGW. To gain more insights into the rheological behavior of samples based on higher chain concentrations, the frequency dependence of  $G'$  and  $G''$  was examined in water and in FGW

at  $20\text{ }^{\circ}\text{C}$  for various ranges of concentrations ( $C$  from  $8.1$  to  $26.5\text{ g/L}$  in water and from  $6.6$  to  $26.5\text{ g/L}$  in FGW) (Figure 2A,B, respectively).

Regarding the aqueous samples, at  $C = 8.1\text{ g/L}$ ,  $G'$  is higher than  $G''$  within the entire detected frequency range, but the moduli remain sensitive to the frequency, by following a relatively close frequency dependence ( $G'$  and  $G'' \propto f^{0.4}$ ) which is typical of a transition toward a solid-like behavior.<sup>13</sup> For higher concentrations, the samples behave as physical gels as  $G'$  is significantly larger (about 1 order of magnitude) than  $G''$  with no strong variation of both moduli with frequency.  $G'$  reaches  $\sim 5000\text{ Pa}$  at  $C = 26.5\text{ g/L}$  (Figure 2A), which is consistent with values reported in the literature ( $2000$  and  $7000\text{ Pa}$  for  $20$  and  $30\text{ g/L}$ , respectively).<sup>7</sup> For FGW-based samples, the viscoelastic response is different. The gel point ( $G' \propto G'' \propto f^{0.4}$ ) was observed to occur at higher concentration ( $C = 10.5\text{ g/L}$ ). Above this concentration, physical gels, characterized by a high  $G'/G''$  ratio, are obtained and the previous “weak gels”, as classified by Clark and Ross-Murphy, shift to more cohesive gels when the polysaccharide concentration increases.<sup>14</sup> It is well accepted in the literature that the gelation of  $\kappa$ -carrageenan in water results from the formation of double-stranded helices laterally arranged in aggregates.<sup>6</sup> From this comparison of the viscoelastic properties, it appears that the critical  $\kappa$ -carrageenan concentration required for the aggregation of helices to occur is higher in FGW than in water. For concentrations above  $20\text{ g/L}$ , the storage moduli in both solvents are quite similar with the  $G'$  value slightly higher in FGW, compared to water (Figure 2B). These striking similarities regarding the overall viscoelastic response suggest similar gelation mechanism in the two solvents. It is well known that the rheological properties of  $\kappa$ -carrageenan hydrogels are thermally sensitive.<sup>7,15</sup> Consequently, the evolution of  $G'$  and  $G''$  as a function of temperature upon successive heating/cooling sweep was evaluated. Additionally, the influence of the polysaccharide

concentration on these transition regions was also examined. From the rheological data at 20 °C, a concentration in  $\kappa$ -carrageenan of 20.5 g/L was selected to study the temperature dependence of  $G'$  and  $G''$  (Figure 3).

Focusing on the hydrogel case, upon heating from 20 °C to 80 °C (dark blue squares, Figure 3),  $G'$  is higher than  $G''$  at 20 °C (as previously shown, see Figure 2A) but in the temperature range between 35 and 55 °C,  $G'$  and  $G''$  sharply decrease of around 3 and 1.5 decade, respectively.  $G''$  becomes greater than  $G'$  for  $T > 48$  °C, indicating a liquid-like behavior. This substantial decrease of both moduli has been ascribed to the thermal-induced dissociation of the helix-based aggregates<sup>16</sup> through the progressive disruption of hydrogen bonds by temperature increase, causing the breakage of the network. The temperature corresponding to the  $G'$  and  $G''$  crossover point, indicator of the gel–solution transition temperature ( $T_{s/g}$ ), was determined to be 48 °C which is consistent with the literature.<sup>7</sup> The viscoelastic response of the hydrogel was then monitored upon an immediate cooling after the first heating ramp. Back at low temperatures, pronounced differences in the  $G'$  and  $G''$  values between the heating and cooling ramp emerge, which come from water evaporation during the analysis. A literature-reported thermal hysteresis phenomenon was ascribed to a different kinetic organization of the polysaccharide helices during heating and cooling, resulting in two different thermal transition temperatures.<sup>17</sup> Figure 3 emphasizes a quite small thermal hysteresis of 3 °C, as a value of  $T_{s/g}$  of 51 °C was recorded (light blue squares). This hysteresis is lower than the one described in the literature, which can reasonably be explained by an overestimation of the  $T_{s/g}$  value due to water evaporation. The FGW-gel, at a similar concentration, was analyzed following the same thermal procedure. As shown in Figure 3, differences in the thermal behavior are observed. First, the decrease of  $G'$  and  $G''$  of the FGW-gel upon the heating ramp is less acute (2 decades against 3 decades in water for  $G'$ ). Second, the decrease of the moduli spreads over a larger range of temperature, with a smooth decrease from 35 to 52 °C followed by a more pronounced one from 52 °C up to 80 °C. Third, the FGW-gel exhibits a better solvent retention propensity: after the two temperature cycles,  $G'$  and  $G''$  are perfectly superimposed, and the initial viscoelastic properties are fully recovered (Figure 3 red and green data points at low temperature). The  $T_{g/s}$  of 74 °C of the FGW-gel, determined upon the heating sweep, is noticeably higher than that in water, and a significant hysteresis (9 °C) appears with a  $T_{s/g}$  identified at 65 °C. The  $T_{s/g}$  values of  $\kappa$ -carrageenan hydrogels are known to decrease while increasing the temperature rate and increase with increasing concentration.<sup>7</sup> Thus, we analyzed two FGW-gels ( $C = 20.5$  and  $26.5$  g/L), at various temperature ramps (1, 2, and 10 °C/min) (Table 1). The global expected trend is observed, but some small discrepancies appear for these values measured from the crossover of  $G'$  and  $G''$ . To complete these data, we also conducted another approach to determine the gelation temperature, based on the divergence of the complex viscosity ( $\eta^*$ ) during the cooling ramp method described in detail by Liu *et al.* for hydrogels (Figure S6).<sup>7</sup> The resulting  $T_{s/g}$  values are quite lower than the ones collected from the crossover method, probably due to the pronounced dispersive character of the thermal transitions within the FGW gels. Interestingly, this series of data better fits with the expected effect of concentration and temperature rate.

**Table 1. Comparison between Two Methods for the Determination of  $T_{s/g}$  Value for Two Concentrations of  $\kappa$ -Carrageenan in FGW ( $C = 20.5$  and  $26.5$  g/L) at Three Different Temperature Ramps (1, 2, and 10 °C/min)<sup>a</sup>**

$\kappa$ -carrageenan concentration	temperature rate (°C/min)	determination of $T_{s/g}$ (°C)	
		method 1 $G'$ and $G''$ crossover	method 2 $\eta^*$
20.5 g/L ( $\approx 1.6$ wt %)	1	88	69
	2	65	68
	10	78	64
26.5 g/L ( $\approx 2.0$ wt %)	1	87	76
	2	70	73
	10	81	71

<sup>a</sup>All experiments were performed at a fixed frequency of 1 Hz with a constant strain of 1%.

Finally, irrespective of the employed method,  $T_{s/g}$  of FGW-gels are higher than the ones measured for the hydrogels. Thus, a higher temperature is required in FGW to allow both the dissociation of helix aggregates and the helix-to-coil transition. Indeed, the high viscosity of the FGW solvent, compared to water, requires a more substantial temperature input to impart a sufficient motion of polysaccharide chains. Additionally, a FGW-gel ( $C = 26.5$  g/L) was subjected to several heating/cooling cycles at 10 °C/min between 40 and 100 °C. These cycles were applied either successively (Figure S7A) or after different waiting times between each cycle (Figure S7B). Figure S7 highlights a complete reversibility of the viscoelastic properties, which underpins that the kinetics of the thermal-induced disorganization/reorganization of the cross-linked zones is rapid and confirms the high solvent retention with temperature for FGW gels, compared to hydrogels.

**3.3. Nanostructure of the Materials.** SAXS measurements were performed to obtain further structural information on the different gels. FGW-gels and hydrogels, at two different chain concentrations ( $C = 8.1$  and  $20.5$  g/L) were analyzed at 20 °C (Figure 4). These concentrations were selected so that the resulting mixtures exhibit different viscoelastic behaviors. Below a polysaccharide concentration of 10 g/L, viscoelastic liquids were obtained in FGW, while “weak” gels started to be formed in water. Conversely, for  $C > 20$  g/L and at 20 °C ( $T < T_{g/s}$ ), physically crosslinked gels characterized by  $G'$  much higher than  $G''$  are generated (see Figure 3). Figure 4A shows the corresponding SAXS patterns [ $I(q)$  vs  $q$ ] of these samples.

All four SAXS profiles presented in Figure 4A can be divided into three parts as a function of the wavevector. For  $q < 0.3$  nm<sup>-1</sup>,  $I(q)$  scales with  $q^{-1}$  in water (Figure 4(A1)). This decrease of the scattering intensity is indicative of the presence of rod-like monodispersed structures,<sup>18</sup> which corroborates the well-accepted gelation mechanism of  $\kappa$ -carrageenan in water that results from the formation of laterally arranged double-stranded helices. Thus, the physical 3D network can be described as made of bound cylinder crosslinks.<sup>6</sup> In FGW at 8.1 g/L of  $\kappa$ -carrageenan, the intensity is somewhat constant in this  $q$ -region, which seems consistent with the fact that this sample is still a viscous liquid composed of only dissolved polysaccharide chains (*i.e.* no bound cylinder crosslinks present yet). In contrast, at 20.5 g/L in FGW, the intensity decreases with a variation of  $q^{-1}$  in a shorter region ( $0.1$  nm<sup>-1</sup>  $< q < 0.3$  nm<sup>-1</sup>) and the slope is steeper at lower  $q$ -values; this result suggests that cylinders are still implied in the structure of the gel but another structure at larger length scales is also expected.

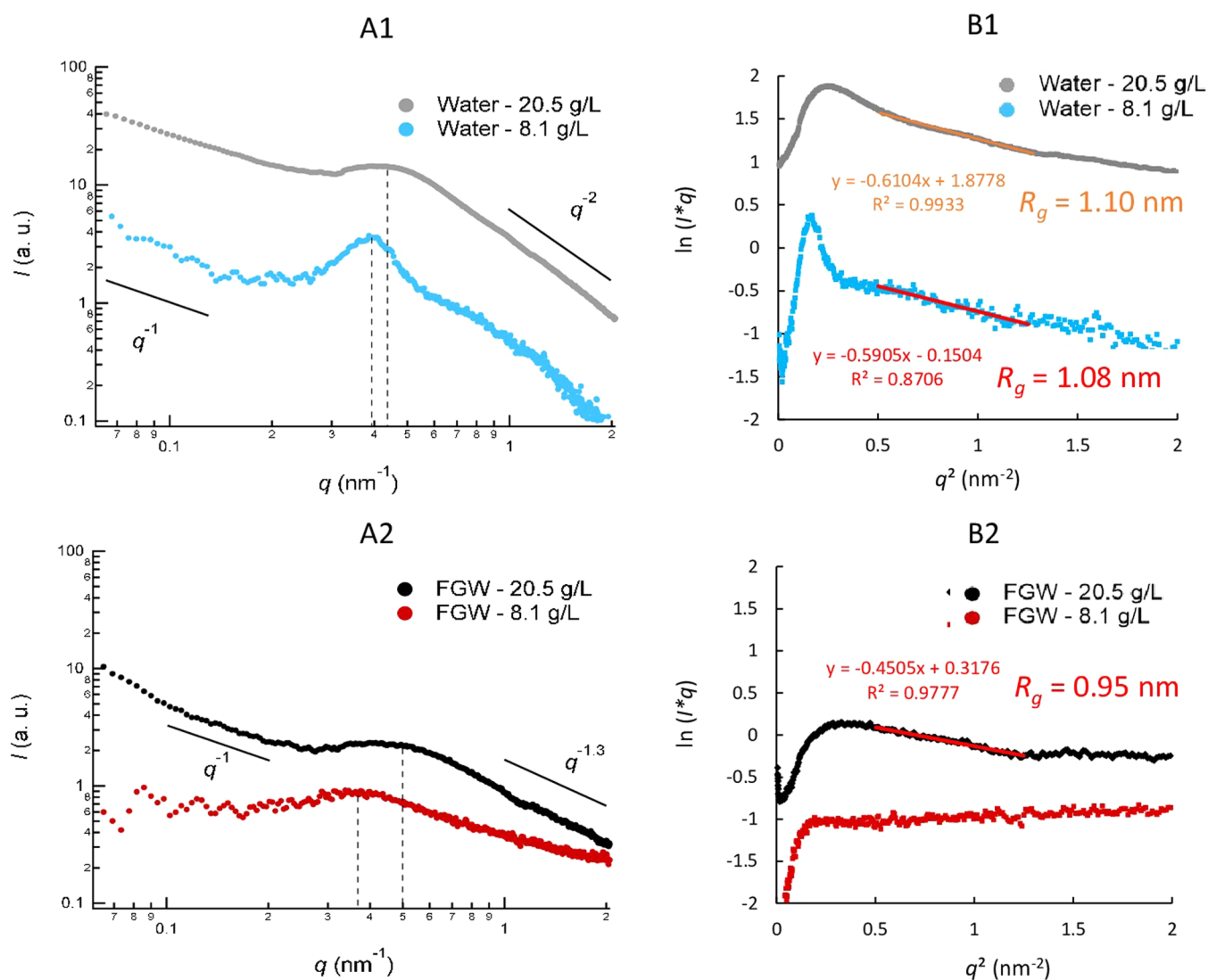


**Figure 4.** (A) SAXS patterns at 20 °C of  $\kappa$ -carrageenan at 8.1 and 20.5 g/L in water (A1) and in FGW (A2). (B) Cross-sectional Guinier plots of the SAXS patterns in water (B1) and in FGW (B2) and graphical exploitation to determine the average cross-sectional radius ( $R_g$ ) of rods composed of aggregates of  $\kappa$ -carrageenan helices.

Then, when  $q$  is comprised between 0.3 and 0.7  $\text{nm}^{-1}$ , scattering patterns are characterized by a broad peak. In the case when water is the solvent, it corresponds to the polyelectrolyte peak of  $\kappa$ -carrageenan.<sup>6</sup> The peak position  $q_{\text{max}}$  is related to the correlation length between chains. As expected, the position of the polyelectrolyte peak is directly linked to the concentration of  $\kappa$ -carrageenan. It is also observed that the polyelectrolyte peak becomes wider when the concentration increases. Nonetheless, by adding progressive amounts of sucrose in 2 wt %  $\kappa$ -carrageenan hydrogels, Yang *et al.* reported that the polyelectrolyte peak vanished for 30 wt % of sucrose. The authors argued that H-bonds between the polysaccharide and the sucrose overcame the electrostatic repulsion interactions between  $\kappa$ -carrageenan chains.<sup>9</sup> In the present study, the continuous phase (FGW) is composed of 50 wt % of fructose and  $\sim 25$  wt % of glycerol and water. Despite the important number of available OH groups of the polysaccharide for developing H-bonds, a structure peak is still observed at  $q$ -values close to those of the polyelectrolyte peak observed for water-based systems. As fructose is strongly H-bonded to glycerol and water, it is less accessible to form H-

bonds with the polysaccharide, as reported by Yang *et al.* for hydrogels containing sucrose.

Finally, when  $q$  becomes larger than 0.7  $\text{nm}^{-1}$ , the decrease of the signal can be assigned to the propensity of the solvent to dissolve polysaccharide free chains. In this region,  $I(q)$  scales with  $q^{-2}$  for water while the exponent is higher for FGW ( $\sim q^{-1.3}$ ). This suggests that the LTTM is a better solvent than water for the  $\kappa$ -carrageenan chains.

To gain more insights into the dimensions of junction zones at the origin of the formation of the physically cross-linked gels, cross-sectional Guinier plots [ $\ln(q \cdot I(q))$  vs  $q^2$ ] were performed. Such representation has often been used in studies reporting the nanostructure of carrageenan hydrogels. Scattering from a long rod with a cross-sectional radius of gyration  $R_g$  is given by the Guinier approximation as  $q \cdot I(q) \approx \exp(-q^2 \cdot R_g^2/2)$ .<sup>19</sup>  $R_g$  can thus be evaluated from the linear region in cross-sectional Guinier plots ( $qR_g < 1$ ). Figure 4B shows the cross-sectional Guinier plots obtained in water and in FGW for the two different studied  $\kappa$ -carrageenan concentrations (8.1 and 20.5 g/L). On the one hand, in the case of water, a linear region appears after the peak due to the

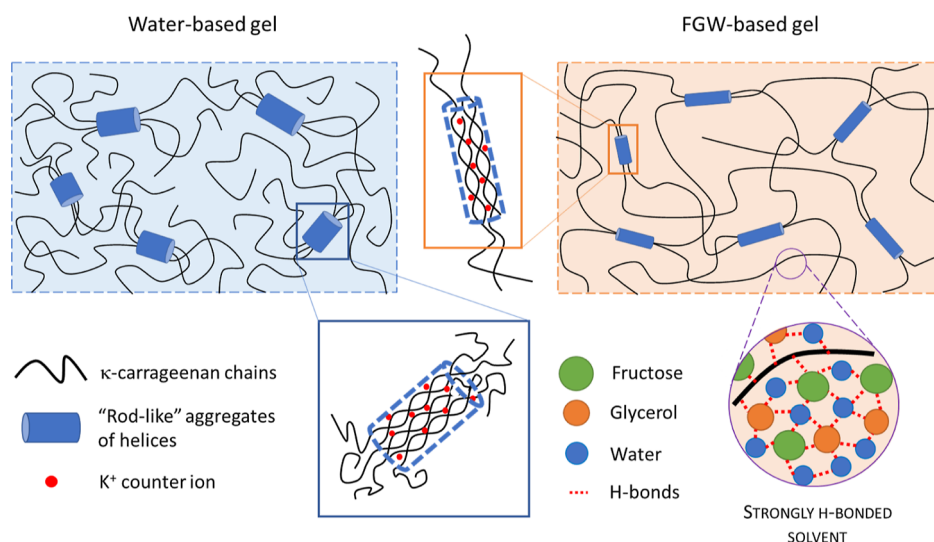


**Figure 5.** Illustration of the suggested organizations obtained in water-based gel and in FGW-based gel.

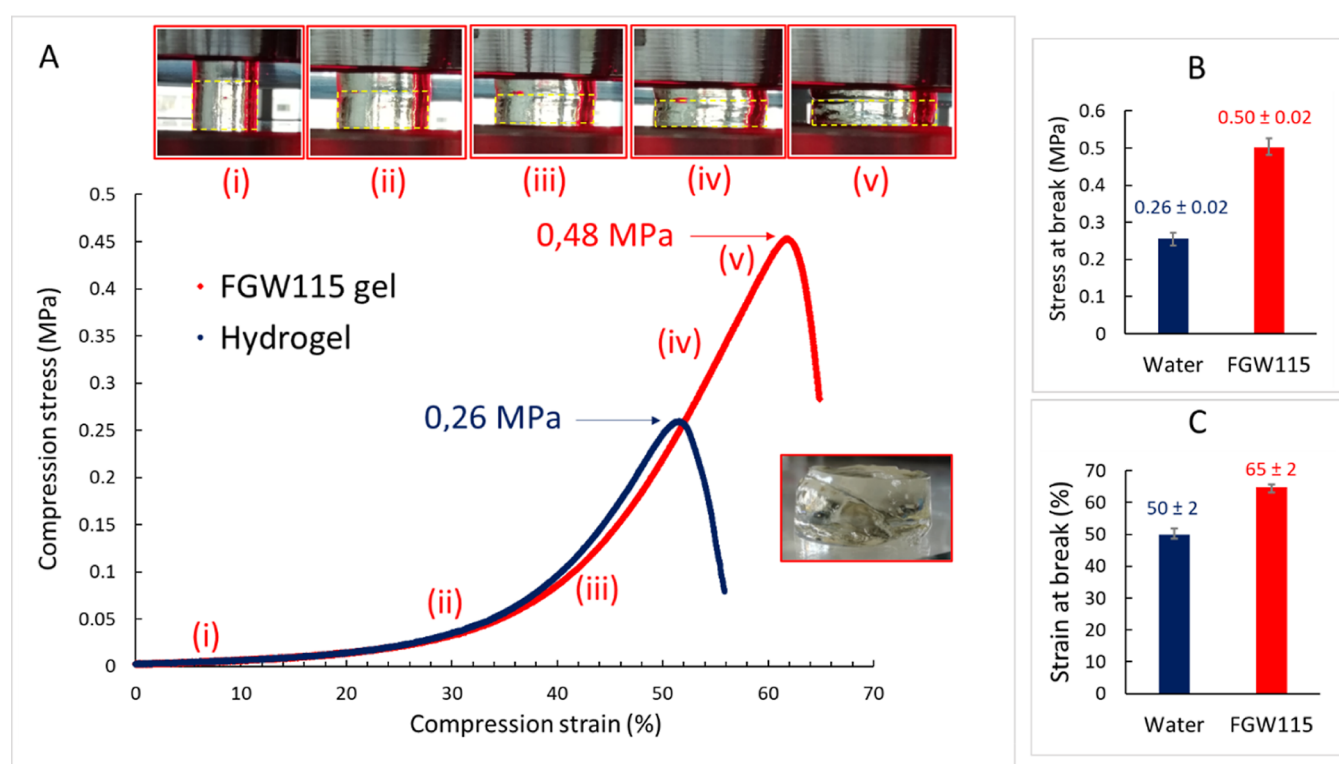


**Figure 6.** (A) Engineering stress–strain curves obtained through compression tests at RT with a compression rate of 1 mm/min for 26.5 g/L gels in water (blue line) and in FGW (red line). (i–v) Pictures of the FGW-gel during compression test are shown to illustrate its ability to reach large compressive deformation. (B) Average stress at break and (C) average strain at break for both solvent-based gels (measurements were performed in triplicate).

electrostatic interactions at lower  $q$  values. The cross-sectional radius of gyration obtained is equivalent to the two concentrations (1.08 and 1.1 nm) (Figure 4(B1)), which is in line with the values reported by Yang *et al.* This result indicates that the number of rods distributed in the aqueous phase increases but the average diameter of the helix aggregates remains constant. On the other hand, Figure 4(B2) shows the cross-sectional Guinier plots obtained in FGW. As discussed before, only rare aggregates may be present in the solution of lowest concentration. Thus, no  $R_g$  value can be determined in this case. Conversely, the Guinier plot for the

FGW gel at  $C = 20.5$  g/L yields a cross-sectional radius of 0.95 nm. SAXS profiles were also investigated at 80 °C for all samples; the Guinier plots obtained at this temperature for  $C = 20.5$  g/L (data not shown) present the same profile as that for the lower concentration in FGW (Figure 4(B2)), suggesting the disappearance of aggregates induced by the temperature increase. This is consistent with rheological measurements and the thermo-reversible behavior of  $\kappa$ -carrageenan gels (Figure 3). Eventually, it appears once again that the gelation mechanism resulting from the formation of laterally arranged double-stranded helices is quite similar between FGW and

water solvents, leading to a rod-like structure with similar size. Since the structure peak of the polysaccharide is broader in FGW, the distribution of interaction lengths is less dispersed in space in the case of water. We thus propose, in Figure 5, the following schematic representation of the internal organization of the hydrogel and FGW gels, mainly based on SAXS investigation but corroborated by the observed rheological behavior. In both gels, gelation is obtained, at low temperature and for sufficient polysaccharide concentration, when  $\kappa$ -carrageenan chains start forming rod-like aggregates acting like physical crosslinks. These physically bounded cylinders (schematized in blue in Figure 5) are made of an aggregate of double-stranded helices.<sup>6</sup> In the case of water-based gels, these aggregates are slightly larger in diameter than for FGW-based gels, with probably one extra double-stranded helix. Another difference between the two systems raises from the interactions between the solvent and the free  $\kappa$ -carrageenan chains, while in the case of hydrogels, the chains are more coiled up; in the case of FGW, being a better solvent for  $\kappa$ -carrageenan chains, it leads to a more extended network with more H-bonds between the solvent and chains, despite an apparently less homogeneous distribution of interactions lengths. With this overall structural picture and considering a same concentration  $\kappa$ -carrageenan chain, the FGW-based gel should lead to a better-connected network with more physical junctions (as the physical aggregates in the hydrogel case involved more  $\kappa$ -carrageenan helices) and stronger solvent–chain interactions (*i.e.* strongly H-bonded solvent).

**3.4. Mechanical Properties.** It was reported that  $\kappa$ -carrageenan forms rigid and brittle hydrogels. When the water phase is modified or another solvent than water is used to obtain  $\kappa$ -carrageenan gels, small deformation tests are used to discuss the viscoelastic behavior of such mixtures. However, the mechanical response to large deformation is scarcely described. Herein, we submitted gels obtained in FGW and in water (26.5 g/L) to compression tests in order to reach the large strain response (see Section 2.3.4 Compression Tests).

Figure 6 regroups the engineering stress–engineering strain curves obtained. As shown in this figure, samples are progressively deformed until a maximum stress is reached, corresponding to the stress at which the gel ruptures. When samples are subjected to small strain (<20%), the mechanical response of the hydrogel and FGW-gel is similar. This is consistent with the rheological measurements performed at small strains (see Figure 2,  $C = 26.5$  g/L): the storage modulus values obtained in both solvents are comparable. Then, for larger strains, the non-linear elastic regime of gels appears. The slope values for both solvents are relatively equivalent, indicating a similar strain-hardening capacity, underlining a relatively analogous physically crosslinked gel structure. However, the range of stress supported by the FGW-gel is significantly higher than that of the hydrogel. In other words, the stress at fracture obtained in FGW (0.50 MPa) is almost twice bigger than that of the hydrogel (0.26 MPa) (Figure 6B). Concomitantly, a higher strain at break is also reported for the FGW-gel compared to the hydrogel, respectively around 65 and 50%, based on triplicate measurements (Figure 6C). For the hydrogel, the values of stress–strain at break are consistent with a previous study that reported a fracture stress of around 0.2 MPa for a 2%  $\kappa$ -carrageenan hydrogel.<sup>20</sup> In the case of FGW, despite the high compression ratio, the gel hardly exudes (compared to water), highlighting again the good solvent retention ability of the system. As the assumption of

constant volume being almost respective, the true stress–true strain curves are given in Figure S8. Figure S8 shows that the true strain of the FGW-gel presents a slight inflexion at large strains indicating a propensity to shear localization before rupture.

Thus, with a very simple preparation method, the FGW mixture proposed in this study appears as an interesting alternative to develop fully biobased gels with enhanced mechanical properties compared to hydrogels. Better properties may arise in the future for FGW-gels as Cairns *et al.* also studied the addition of carob gum to obtain tougher  $\kappa$ -carrageenan hydrogels which were better able to withstand mechanical stress.<sup>20</sup>

## 4. CONCLUSIONS

In conclusion, we were able to develop fully biosourced physical gels through the incorporation of  $\kappa$ -carrageenan chains in the FGW solvent, *via* an eco-friendly experimental approach. As hypothesized in the introduction, FGW-based gels present improved properties compared to their aqueous analogues. Indeed, the gels exhibit promising thermal behavior with an extended operating temperature range compared to hydrogels. Even if the study of the nanostructure and the rheological characterizations evidenced a similar gelation mechanism of  $\kappa$ -carrageenan in both solvents, the transition temperatures  $T_{g/s}$  of the FGW-gels are higher than the ones obtained in water and the initial viscoelastic properties are fully recovered after multiple heating and cooling cycles, which is a key advantage compared to hydrogels. The supramolecular FGW structuration offers a better solvent retention and contributes to the formation of additional H-bonds within the gel. This peculiar spatial structuration provides a mechanical response improvement demonstrated by compression tests. Finally, we validate through this study that the enhanced properties of these FGW-based gels result from the formation of synergetic interactions between this peculiar LTTM solvent and  $\kappa$ -carrageenan polymer chains. These soft materials, never reported in the literature so far, are expected to find applicative uses in green and sustainable soft material technologies.

## ■ ASSOCIATED CONTENT

### Supporting Information

The Supporting Information is available free of charge at <https://pubs.acs.org/doi/10.1021/acssuschemeng.2c04437>.

Additional polysaccharide characterizations (TGA, SEC, and NMR) and complementary physico-chemical analysis of the gels: thermal properties (DSC) and rheological and mechanical properties (PDF)

## ■ AUTHOR INFORMATION

### Corresponding Author

Aurélia Charlot – Université Lyon, CNRS, Université Claude Bernard Lyon 1, INSA Lyon, Université Jean Monnet, UMR 5223, Ingénierie des Matériaux Polymères, F-69621 Villeurbanne Cedex, France; [orcid.org/0000-0002-8743-7752](https://orcid.org/0000-0002-8743-7752); Phone: +33 (0)4 72 43 63 38; Email: [aurelia.charlot@insa-lyon.fr](mailto:aurelia.charlot@insa-lyon.fr)

### Authors

Benoit Caprin – Université Lyon, CNRS, Université Claude Bernard Lyon 1, INSA Lyon, Université Jean Monnet, UMR 5223, Ingénierie des Matériaux Polymères, F-69621

Villeurbanne Cedex, France; Gattefossé SAS, 69804 Saint-Priest Cedex, France

**Guadalupe Viñado-Buil** – Université Lyon, CNRS, Université Claude Bernard Lyon 1, INSA Lyon, Université Jean Monnet, UMR 5223, Ingénierie des Matériaux Polymères, F-69621 Villeurbanne Cedex, France

**Guillaume Sudre** – Université Lyon, CNRS, Université Claude Bernard Lyon 1, INSA Lyon, Université Jean Monnet, UMR 5223, Ingénierie des Matériaux Polymères, F-69621 Villeurbanne Cedex, France

**Xavier P. Morelle** – Université Lyon, CNRS, Université Claude Bernard Lyon 1, INSA Lyon, Université Jean Monnet, UMR 5223, Ingénierie des Matériaux Polymères, F-69621 Villeurbanne Cedex, France

**Fernande Da Cruz-Boisson** – Université Lyon, CNRS, Université Claude Bernard Lyon 1, INSA Lyon, Université Jean Monnet, UMR 5223, Ingénierie des Matériaux Polymères, F-69621 Villeurbanne Cedex, France

**Etienne Fleury** – Université Lyon, CNRS, Université Claude Bernard Lyon 1, INSA Lyon, Université Jean Monnet, UMR 5223, Ingénierie des Matériaux Polymères, F-69621 Villeurbanne Cedex, France; [orcid.org/0000-0003-0592-9700](https://orcid.org/0000-0003-0592-9700)

Complete contact information is available at:  
<https://pubs.acs.org/10.1021/acssuschemeng.2c04437>

## Notes

The authors declare no competing financial interest.

## ACKNOWLEDGMENTS

This project has received funding from Gattefossé. The authors are also thankful to Agnès Crepet (IMP, Université Claude Bernard Lyon 1) for her valuable help to obtain and process size exclusion chromatography and to all technical support received at the IMP lab to achieve this work. The authors also acknowledge the D2AM beamline staff at ESRF and are in debt to Isabelle Morfin (LIPhy, Grenoble) for the setup of the beamline and the initial data treatment.

## REFERENCES

- (1) Tomé, L. C.; Mecerreyes, D. Emerging Ionic Soft Materials Based on Deep Eutectic Solvents. *J. Phys. Chem. B* **2020**, *124*, 8465–8478.
- (2) Depoorter, J.; Mourlevat, A.; Sudre, G.; Morfin, I.; Prasad, K.; Serghei, A.; Bernard, J.; Fleury, E.; Charlot, A. Fully Biosourced Materials from Combination of Choline Chloride-Based Deep Eutectic Solvents and Guar Gum. *ACS Sustainable Chem. Eng.* **2019**, *7*, 16747–16756.
- (3) Zeng, C.; Zhao, H.; Wan, Z.; Xiao, Q.; Xia, H.; Guo, S. Highly biodegradable, thermostable eutectogels prepared by gelation of natural deep eutectic solvents using xanthan gum: Preparation and characterization. *RSC Adv.* **2020**, *10*, 28376–28382.
- (4) Xia, H.; Ren, M.; Zou, Y.; Qin, S.; Zeng, C. Novel Biocompatible Polysaccharide-Based Eutectogels with Tunable Rheological, Thermal, and Mechanical Properties: The Role of Water. *Molecules* **2020**, *25*, 3314.
- (5) Zia, K. M.; Tabasum, S.; Nasif, M.; Sultan, N.; Aslam, N.; Noreen, A.; Zuber, M. A review on synthesis, properties and applications of natural polymer based carrageenan blends and composites. *Int. J. Biol. Macromol.* **2017**, *96*, 282–301.
- (6) Yuguchi, Y.; Thu Thuy, T. T.; Urakawa, H.; Kajiwara, K. Structural characteristics of carrageenan gels: temperature and concentration dependence. *Food Hydrocolloids* **2002**, *16*, 515–522.

(7) Liu, S.; Huang, S.; Li, L. Thermoreversible gelation and viscoelasticity of  $\kappa$ -carrageenan hydrogels. *J. Rheol.* **2016**, *60*, 203–214.

(8) Yang, Z.; Yang, H.; Yang, H. Characterisation of rheology and microstructures of  $\kappa$ -carrageenan in ethanol-water mixtures. *Food Res. Int.* **2018**, *107*, 738–746.

(9) Yang, Z.; Yang, H.; Yang, H. Effects of sucrose addition on the rheology and microstructure of  $\kappa$ -carrageenan gel. *Food Hydrocolloids* **2018**, *75*, 164–173.

(10) Caprin, B.; Charton, V.; Rodier, J.-D.; Vogelgesang, B.; Charlot, A.; Da Cruz-Boisson, F.; Fleury, E. Scrutiny of the supramolecular structure of bio-sourced fructose/glycerol/water ternary mixtures: Towards green low transition temperature mixtures. *J. Mol. Liq.* **2021**, *337*, 116428.

(11) Caprin, B.; Charton, V.; Vogelgesang, B. Chapter Twelve—The use of NADES to support innovation in the cosmetic industry. In *Advances in Botanical Research: Eutectic Solvents and Stress in Plants*; Academic Press, 2021; Vol. 97, pp 309–332.

(12) Mangione, M. R.; Giacomazza, D.; Bulone, D.; Martorana, V.; San Biagio, P. L. Thermoreversible gelation of  $\kappa$ -Carrageenan: relation between conformational transition and aggregation. *Biophys. Chem.* **2003**, *104*, 95–105.

(13) Richter, S. Recent Gelation Studies on Irreversible and Reversible Systems with Dynamic Light Scattering and Rheology - A Concise Summary. *Macromol. Chem. Phys.* **2007**, *208*, 1495–1502.

(14) Clark, A. H.; Ross-Murphy, S. B. Structural and mechanical properties of biopolymer gels. In *Biopolymers*; Advances in Polymer Science; Springer-Verlag, 1987; pp 57–192.

(15) Mangione, M. R.; Giacomazza, D.; Bulone, D.; Martorana, V.; Cavallaro, G.; San Biagio, P. L. K(+) and Na(+) effects on the gelation properties of kappa-Carrageenan. *Biophys. Chem.* **2005**, *113*, 129–135.

(16) Rochas, C.; Rinaudo, M. Mechanism of gel formation in  $\kappa$ -carrageenan. *Biopolymers* **1984**, *23*, 735–745.

(17) Ueda, K.; Itoh, M.; Matsuzaki, Y.; Ochiai, H.; Imamura, A. Observation of the Molecular Weight Change during the Helix–Coil Transition of  $\kappa$ -Carrageenan Measured by the SEC–LALLS Method. *Macromolecules* **1998**, *31*, 675–680.

(18) Hollamby, M. J. Practical applications of small-angle neutron scattering. *Phys. Chem. Chem. Phys.* **2013**, *15*, 10566–10579.

(19) *Small Angle X-ray Scattering*; Glatter, O., Kratky, O., Eds.; Academic Press: London, 1982; p 515.

(20) Cairns, P.; Morris, V. J.; Miles, M. J.; Brownsey, G. J. Comparative studies of the mechanical properties of mixed gels formed by kappa carrageenan and tara gum or carob gum. *Food Hydrocolloids* **1986**, *1*, 89–93.